Research Square

Preprints are preliminary reports that have not undergone peer review.
They should not be considered conclusive, used to inform clinical practice,
or referenced by the media as validated information.

Thylakoid K+-permeable channel required for photosynthesis reveals a conserved role of bestrophins

Shin Hamamoto

uhamamoto@g.ecc.u-tokyo.ac.jp

The University of Tokyo https://orcid.org/0000-0001-7619-572X

Haruhiko Jimbo

Saitama University

Kaisei Maeda

Institute of Science Tokyo

Keitaro Tanoi

The University of Tokyo https://orcid.org/0000-0001-7545-2771

Kan Tanaka

Institute of Science Tokyo

Hisashi Kawasaki

The University of Tokyo https://orcid.org/0000-0001-6662-9301

Article

Keywords: bestrophin, K+ channel, thylakoid, photosynthesis, Synechocystis sp. PCC 6803

Posted Date: May 6th, 2026

DOI: https://doi.org/10.21203/rs.3.rs-6268488/v1

License: This work is licensed under a Creative Commons Attribution 4.0 International License.
Read Full License

Additional Declarations: There is **NO** Competing Interest.

Thylakoid K^+-permeable channel required for photosynthesis reveals a conserved role of bestrophins

Shin Hamamoto[1,4#], Haruhiko Jimbo[2], Kaisei Maeda[3], Keitaro Tanoi[1], Kan Tanaka[3], Hisashi Kawasaki[1,4#]

[1]Department of Applied Biological Chemistry, Graduate School of Agricultural and Life Sciences, The University of Tokyo, Bunkyo-ku, Tokyo, 113-8657, Japan.

[2]Engineering and Institute for Environmental Science and Technology, Saitama University, 255 Shimo-Okubo, Sakura-ku, Saitama, 338-8570, Japan

[3]Laboratory for Chemistry and Life Science, Institute of Innovative Research, Institute of Science Tokyo, Yokohama, 226-8501 Japan

[4] Collaborative Research Institute for Innovative Microbiology, The University of Tokyo, 1-1-1, Yayoi, Bunkyo-ku, Tokyo, 113-8657, Japan

#Correspondence: Hisashi Kawasaki (email: ukawasaki@g.ecc.u-tokyo.ac.jp)

#Correspondence: Shin Hamamoto (email: uhamamoto@g.ecc.u-tokyo.ac.jp)

Keywords: bestrophin, K^+ channel, thylakoid, photosynthesis, *Synechocystis* sp. PCC 6803

Research on thylakoid membrane transport proteins that regulate photosynthetic activity has predominantly focused on *Arabidopsis thaliana*, where these proteins have been shown to modulate photosynthesis in response to changes in light intensity. However, our

understanding of transport proteins in cyanobacteria remains limited. Here, we focused on the ion channel Sll1024, localized within the thylakoid membrane of *Synechocystis* sp. PCC 6803. The Δ*sll1024* mutant exhibited delayed growth and a marked reduction in photosynthetic efficiency under low K^+ conditions. Electrophysiological analyses confirmed that Sll1024 is a K^+ permeable channel. Together with the reported substantial K^+ permeability of the plant bestrophin AtVCCN1, our findings raise the possibility that thylakoid bestrophin-type channels in both cyanobacteria and plants contribute physiologically to K^+ flux across the thylakoid membrane, which may occur in either direction depending on the prevailing physiological and electrochemical conditions. These results provide insight into the role of Sll1024 and support the idea that K^+ permeation by thylakoid bestrophins contributes to the maintenance of photosynthetic performance. The absence of Sll1024 led to a more pronounced decrease in photosynthetic performance than previously characterized K^+ and anion transporters, underscoring its potential importance in optimizing cyanobacterial photosynthesis for large-scale, solar energy-driven biotechnological applications. Photosynthesis is a critical metabolic process that generates oxygen and carbohydrates by converting light energy into chemical energy through electron transport reactions in the thylakoid membrane[1]. During light-dependent reactions, photosystem II (PSII) absorbs photons, resulting in the splitting of water molecules into oxygen, protons, and electrons. These electrons are transferred via the electron transport chain, which includes plastoquinone, cytochrome b_6f, and photosystem I (PSI), ultimately leading to the production of NADPH. Proton transport across the thylakoid membrane generates a proton motive force (pmf) that drives ATP synthesis via ATP synthase[2]. Under excessive light conditions, reactive oxygen species can accumulate, risking damage to the photosynthetic apparatus through

photoinhibition[3]. To mitigate this, plants have developed protective mechanisms such as non-photochemical quenching (NPQ), which dissipates excess energy as heat[4]. NPQ is closely associated with the proton gradient (ΔpH) across the thylakoid membrane, which constitutes the pmf alongside the electric potential (Δψ).

Ion transporters are pivotal in modulating the balance between ΔpH and Δψ. Extensive research in *Arabidopsis thaliana* has demonstrated the roles of ion transport proteins, such as KEA3 and AtVCCN1, in fine-tuning photosynthetic regulation[5–8]. AtVCCN1 has mainly been characterized as a voltage-dependent Cl^- channel; however, planar lipid bilayer analysis also revealed a non-negligible K^+ permeability[7]. In contrast, information on ion transporters in cyanobacteria is limited. Thus, this present study aimed to investigate the bestrophin-like protein Sll1024 in *Synechocystis* sp. PCC 6803, highlighting its localization to the thylakoid membrane, its critical role in photosynthesis, and its possible relevance to a conserved K^+-flux function of thylakoid bestrophin channels.

Bestrophin ion channels are highly conserved across diverse organisms, including animals, plants, and microorganisms[9–11]. The *sll1024* gene, conserved in the genome of *Synechocystis* sp. PCC 6803 belongs to this family of bestrophin channels. Upon investigating the conservation of bestrophins in cyanobacteria, homologs of Sll1024 were identified across multiple genera and orders (Supplementary Table 1 and Supplementary Fig. 1), indicating that this channel family is widely distributed and may play a marked physiological role in cyanobacteria.

KpBest1 from *Klebsiella pneumoniae* is the only prokaryotic bestrophin channel for which the three-dimensional structure has been determined[11]. Functional analyses using electrophysiological techniques have shown that KpBest1, despite being a bestrophin

channel, facilitates cation transport. When comparing the protein sequences of Sll1024 and KpBest1, 30% identity and 71% similarity were found. However, Sll1024 lacks the ATP-binding domain found in mammalian bestrophins and KpBest1, as well as the Ca^{2+}-binding domain widely conserved in mammalian bestrophins, which is also absent in KpBest1[11–13]. Notably, Sll1024 contains an amino acid selectivity filter of KpBest1, suggesting that Sll1024 may likewise mediate cation transport (Supplementary Fig. 2).

To further elucidate the physiological role of Sll1024 in *Synechocystis* sp. PCC 6803, an *sll1024* deletion mutant was generated, and its phenotype was analyzed (Supplementary Fig. 3a). When *Synechocystis* sp. PCC 6803 was cultured under K^+-limited conditions (33 μM KCl), the wild-type (WT) strain showed normal growth, while the Δ*sll1024* strain exhibited remarkably slower growth. Adding 100 μM or 500 μM KCl to the medium restored the growth of the Δ*sll1024* strain to levels comparable to the WT (Fig. 1a), suggesting that Sll1024 may be involved in K^+ uptake from the extracellular environment or its transport across the thylakoid membrane. The plasma membrane-localized Kdp and Ktr transporters facilitate extracellular K^+ uptake in *Synechocystis* sp. PCC 6803[14,15]. As these transporters are already known to mediate K^+ uptake at the plasma membrane, Sll1024 is possibly not involved in extracellular space seems unlikely. Instead, Sll1024 functions plausibly within the thylakoid membrane.

To confirm the intracellular localization of Sll1024 in *Synechocystis* sp. PCC 6803, membrane fractions were prepared, and Sll1024 was detected using immunoblotting. A transformant harboring a His-tag sequence and a kanamycin resistance gene at the 3' end of the *sll1024* gene was constructed (Supplementary Fig. 3b). Immunoblotting using an anti-His-tag antibody revealed that Sll1024 was exclusively present in the thylakoid membrane fraction (Fig. 1b). The weak signal suggests that Sll1024 is expressed at very

low levels and is likely under tight regulation. The thylakoid localization of Sll1024, similar to that of the homologous VCCN1 channel in plants, suggests its involvement in ion transport within the thylakoid membrane, potentially contributing to the regulation of photosynthesis.

Given the specific localization of Sll1024 to the thylakoid membrane, as well as the localization of its homolog VCCN1 to the thylakoid membrane in plant chloroplasts, we investigated whether Sll1024 contributes to photosynthetic activity. To assess this, the photosynthetic activity of WT and Δ*sll1024* strains grown in a BG-11 medium containing 33 μM KCl was measured using an oxygen electrode. Under these conditions, both the net photosynthetic activity and electron transport rate (ETR) of the Δ*sll1024* strain were significantly lower compared to those of the WT. However, when 100 μM KCl was added to the medium, both the net photosynthetic activity and ETR of the Δ*sll1024* strain restored to levels comparable to those of the WT (Fig. 1c). Notably, the activity of PSII remained unchanged between the WT and Δ*sll1024* strains, regardless of the presence of KCl (Fig. 1c). These results suggest that Sll1024, localized to the thylakoid membrane, plays a role in regulating photosynthetic activity, likely downstream of PSII within the electron transport chain.

To further analyze the function of Sll1024 in *Synechocystis* sp. PCC 6803, eliminating the background activity of other ion transport proteins in the thylakoid membrane is essential. However, due to the limited information available on these transporters, constructing such knockout strains is highly challenging. Thylakoid-localized and other organelle-localized proteins can be heterologously expressed and functionally characterized in the plasma membrane of *Escherichia coli*[16–18]. Building on these findings, we employed *E. coli* as a heterologous expression system to investigate the function of

Sll1024. Due to the difference in codon usage frequencies between *Synechocystis sp.* PCC 6803 and *Escherichia coli*, the *sll1024* gene was optimized by converting it to codons frequently used in *E. coli* to enhance its expression efficiency. The optimized *sll1024* gene was then cloned into an *E. coli* expression vector (Supplemental Fig. 4). A K^+ uptake-deficient strain of *E. coli* was generated by knocking out genes encoding K^+ transporters such as KdpABC, KUP, TrkG, and TrkH[19,20]. When *sll1024* was introduced into this strain, the Sll1024-expressing strain complemented the growth deficiency in K^+-limited media (15 mM KCl) (Fig. 2a). Furthermore, K^+ uptake experiments showed that the Sll1024-expressing strain up took more K^+ compared to a control strain carrying an empty vector (EV; Fig. 2b). These results indicate that Sll1024 is functionally expressed in the plasma membrane of *E. coli* and can transport K^+.

We further examined the transport activity of Sll1024 through electrophysiological experiments. Using the spheroplast incubation method, we enlarged the Sll1024-expressing *E. coli* strain and measured the Sll1024-derived channel current using the whole-cell recording mode of the patch-clamp method[21–23]. When a voltage ranging from −80 to 80 mV was applied, the Sll1024-expressing strain exhibited larger currents than the control strain (Fig. 2c). The ion current derived from Sll1024 showed currents in both positive and negative directions and exhibited weak voltage dependency (Fig. 2c). To determine ion selectivity, we replaced the bath buffer with one containing 30 mM KCl while maintaining the pipette buffer as described above (Fig. 2d and e). In the Sll1024-expressing strain, the reversal potential shifted to −7.7 mV, whereas the EV strain only exhibited a shift of −3.0 mV. These results suggest that Sll1024-expressing strain has a higher selectivity for cations over anions, as compared to the EV strain. The theoretical shift width for a transporter selectively transporting only cations is approximately −30

mV, indicating that while Sll1024 favors cations, it also exhibits some transport activity for anions.

Finally, we examined the single-channel conductance of Sll1024 using outside-out patch-clamp recordings. With pipette and bath buffers containing 100 mM KCl, the inward current exhibited a conductance of 206 pS, while the outward current displayed a conductance of 154 pS (Fig. 2f and g). These findings provide further evidence of ion transport capabilities of Sll1024, supporting its role in K^+ transport and its involvement in photosynthetic activity regulation in *Synechocystis* sp. PCC 6803.

We investigated the ultrastructure of the thylakoid membrane in the Δ*sll1024* mutant using transmission electron microscopy. In the Δ*sll1024* cells, an expansion of the thylakoid lumen was observed in many, but not all, cells. The thylakoid lumen of Δ*sll1024* appeared transparent, likely due to its low electron density (Fig. 3a–c, Supplementary Fig. 5). To quantify this observation, image analysis was performed to measure the width of the thickest part of the lumen. While the lumen in WT cells measured approximately 6 nm, the lumen in Δsll1024 cells was significantly wider, measuring approximately 20 nm. A similar expansion has been observed in *atvccn1* mutant cells; however, the molecular mechanisms underlying such phenomena remain unclear[10].

An increasing number of studies indicate that ion transporters and ion channels localized in the thylakoid membrane play a significant role in photosynthetic activity[5–7]. The bestrophin channel AtVCCN1, for example, has been described as a voltage-dependent Cl^- channel and is involved in regulating photosynthetic responses to changes in light conditions by suppressing increases in $\Delta\psi$[7,10,24]. Importantly, planar lipid bilayer experiments also detected a non-negligible permeability of AtVCCN1 to K^+[7]. KpBest1,

the first reported bacterial bestrophin to be characterized, is likewise notable in functioning as a cation channel rather than an anion channel, sparking interest in the physiological role of Sll1024, a bacterial-type bestrophin in *Synechocystis* sp. PCC 6803, particularly in relation to photosynthesis and its ion channel function.

Our findings show that Δ*sll1024* grows poorly at low KCl concentrations relative to the WT. However, supplementation with KCl restored the growth of Δ*sll1024* to levels comparable to WT (Fig. 1a). Likewise, the photosynthetic activity of Δ*sll1024* was significantly reduced in the absence of KCl but was restored to WT levels upon KCl supplementation (Fig. 1c). Localization studies confirmed that Sll1024 is specifically expressed in the thylakoid membrane and is absent from the cytoplasmic membrane (Fig. 1b). Together, these observations indicate that the rescue of growth and photosynthetic activity by KCl is more likely to reflect regulation of K^+ or Cl^- concentrations within the stroma and thylakoid lumen than direct uptake of K^+ or Cl^- from the external environment into the cell.

The key question remains whether Sll1024 primarily facilitates the transport of K^+ or Cl^-. Given that the BG-11 medium used in our experiments contains sufficient Cl^- (260–270 μM), the changes in K^+ concentrations possibly had a more pronounced effect than Cl^- levels, which were modified by adding KCl. Electrophysiological analyses of Sll1024 using a heterologous expression system in *E. coli* demonstrated that Sll1024 can transport both K^+ and Cl^-, but with a higher selectivity for K^+ over Cl^-, as indicated by the shift in reversal potential (Fig. 2d and e). Collectively, these results suggest that Sll1024 plays a significant role in regulating photosynthetic activity through K^+ transport. Previous studies have indicated K^+ transport from the thylakoid lumen to the stroma in response to fluctuating light conditions, although the responsible transport proteins had not been

previously identified[25–28]. Our study identifies Sll1024 as the first transport protein that matches the characteristics of a K^+ transporter in the thylakoid membrane.

One attractive possibility is that the substantial K^+ permeability reported for AtVCCN1 is not merely a minor biophysical feature, but instead reflects a physiologically relevant property shared by thylakoid bestrophin channels. Considered together with the K^+ permeability of Sll1024 shown here and the K^+-dependent phenotype of the Δ*sll1024* mutant, these observations support the hypothesis that K^+ movement across the thylakoid membrane is an important component of bestrophin channel function in both cyanobacteria and plants. In this view, the physiological role of thylakoid bestrophins may not be explained solely by anion conductance; rather, a modest but strategically positioned K^+ permeability could help shape osmotic balance, modulate the proton motive force, and sustain efficient electron transport.

The thylakoid lumen was markedly expanded in Δ*sll1024* relative to the WT, a phenotype that has also been reported in plants under moderate light conditions [29–31]. Changes in thylakoid lumen volume are thought to affect photosynthetic electron transport, photoprotection, and PSII repair. Ion flux, particularly K^+ movement from the lumen to the stroma, may regulate osmotic pressure within the thylakoid lumen, preventing excessive swelling during photosynthesis. This interpretation is consistent with the possibility that the substantial K^+ permeability of AtVCCN1 is physiologically meaningful, and that Sll1024 and AtVCCN1 share a conserved role in controlling lumenal osmotic balance through K^+ flux across the thylakoid membrane. The direction and physiological contribution of this flux remain unclear in both *Synechocystis* sp. PCC 6803 and plant chloroplasts, and defining these parameters should provide further insight into the role of K^+ in photosynthetic regulation. In addition, our functional analysis was

217 performed with Sll1024 expressed in the *E. coli* membrane. Because thylakoid
218 membranes are rich in glycolipids, unlike the *E. coli* membrane, the activation properties
219 of Sll1024 in its native membrane environment may differ from those observed in the *E.*
220 *coli* membrane. Establishing new measurement systems, such as patch-clamp
221 measurement directly on thylakoid membranes, should help to resolve these issues.
222 In our study, the net photosynthetic activity and ETR from PSII to PSI were significantly
223 reduced in the Δ*sll1024* strain under conditions without KCl supplementation (Fig. 1c).
224 Because PSII activity itself was only weakly affected, these results suggest that Sll1024
225 supports photosynthetic efficiency by influencing components of the electron transport
226 chain downstream of PSII (Supplementary Fig. 6). In *A. thaliana*, ion transporters such
227 as KEA3, VCCN1, and CLCe contribute to acclimation under fluctuating light. However,
228 the photosynthetic defect of Δ*sll1024* appears more severe than those reported for these
229 plant mutants, suggesting that Sll1024 may regulate photosynthesis through a distinct
230 molecular mechanism, different from these well-characterized thylakoid membrane-
231 localized transporters. Notably, the magnitude of the defect further suggests that K^+
232 transport can exert a more substantial influence on photosynthesis than has been
233 appreciated previously.
234 Cyanobacteria-based cell factories exploit sunlight-driven photosynthesis to produce
235 value-added compounds, and the conservation of Sll1024 across many cyanobacterial
236 species suggests that defining its function could support the rational optimization of these
237 systems, particularly under fluctuating natural light conditions. More broadly, our
238 findings, together with the reported substantial K^+ permeability of the plant thylakoid
239 bestrophin AtVCCN1, raises the possibility that K^+ permeation through thylakoid
240 bestrophin channels represents a conserved mechanism contributing to photosynthetic

homeostasis across oxygenic photosynthetic organisms. In this view, the physiological role of thylakoid bestrophins may not be explained solely by anion conductance; rather, K^+ permeability may help regulate osmotic balance, shape the proton motive force, and sustain efficient photosynthetic electron transport. Because potassium is an essential macronutrient for agriculture, a deeper understanding of how photosynthetic organisms use and regulate K^+ may ultimately help improve potassium-use efficiency. In the longer term, such knowledge may contribute to more efficient fertilizer use and to more stable food production under conditions in which potassium resources and fertilizer access are unevenly distributed.

Materials and methods

Generation of *sll1024* mutant strain and *His-tagged sll1024* expressing strain, and culture conditions

Glucose-tolerant *Synechocystis* sp. PCC 6803 (GT-I) was used as the WT strain, and all transformants were derived from these WT cells. To generate an *sll1024* knockout mutant, DNA fragments corresponding to the 5′ upstream region (0–467 nt) and 3′ downstream region (468–933 nt) of the *sll1024* gene were amplified using PCR with primers F1 and R1, and F2 and R2, respectively. These primers contained 15 bp of additional sequences identical to the chloramphenicol-resistant (*Cm*^{r}) gene. A DNA fragment containing the *Cm*^{r} was amplified using primers F3 and R3. The three amplified DNA fragments were assembled using the NEBuilder Gibson Assembly reaction mix (New England Biolabs, Ipswich, MA, USA) at 50 °C for 30 min. The resulting DNA constructs were then used to transform WT cells, and the segregation of the disrupted *sll1024* gene in the genome

of the transformants was confirmed using PCR with primers F1 and R2.

For the generation of a His-tagged *sll1024* strain, DNA fragments containing the *sll1024* gene and adjacent genomic regions were amplified by PCR using primers F1 and R4, and F5 and R5. These primers contained 15 bp of additional sequences identical to the kanamycin-resistant (*Km*^{r}) gene. A DNA fragment containing the *Km*^{r} gene was amplified using primers F6 and R6. The amplified DNA fragments were assembled in the same manner as for the knockout mutant and used to transform WT cells. All PCR primers used in the construction of gene deletion mutants are listed in Supplementary Table 2.

WT and transformant cells were grown photoautotrophically at 32 °C in a liquid BG-11 medium containing 33 μM KCl under fluorescent light (10 μmol photons m^{-2} s^{-1}) with sterile aeration. Cultures with an optical density at 730 nm (OD_{730}) of 1.0 ± 0.1, corresponding to approximately 4.0 μg Chl mL^{-1}, were used for assays, unless otherwise indicated.

Subcellular localization of His-tagged Sll1024 protein

Cells expressing His-tagged Sll1024 were resuspended in 50 mM HEPES-KOH buffer (pH 7.5) containing a protease inhibitor cocktail (Nakalai Tesque, Japan). Cells were lysed using 0.1 mm Zirconia beads and a beads-beater (Bio Medical Science, Japan) with 20-s intervals on ice. Unbroken cells and cell walls were removed using centrifugation (800 ×*g*, 4 °C, 10 min). Thylakoid membranes were pelleted using centrifugation at 18,000 ×*g* (4 °C, 10 min), while plasma membranes were separated from soluble proteins using centrifugation at 100,000 ×*g* (4 °C, 2 h). Proteins from each cellular fraction were separated using SDS-PAGE on a 12.5% polyacrylamide gel containing 6 M urea and subjected to immunological detection using His-tag-specific antibodies (Medical and Biological Laboratories, Japan). Antibodies against PsbC (AS111787) and SbtA

289 (AS132657) were purchased from Agrisera (Sweden). Immunological detection of EF-
290 Tu was performed as described previously[32].

291 **Measurement of photosynthetic activity**

292 Photosynthetic activity was measured at 32 °C using a Clark-type oxygen electrode
293 (Hansatech Instruments, Norfolk, UK). PSII activity was assessed in the presence of 1
294 mM benzoquinone and 1 mM $K_3Fe(CN)_6$, while net photosynthetic activity was measured
295 with 10 mM $NaHCO_3$, as described previously[33]. The rate of photosynthetic electron
296 transfer was evaluated based on oxygen consumption in the presence of 1 mM methyl
297 viologen and 1 mM KCN, as described previously[34].

298 **Construction of *E. coli* strain**

299 The genes encoding K^+ uptake transporters (kdpA, kup, trkG, and trkH) in the genome
300 of *E. coli* strain W3110 were deleted using the Quick & Easy *E. coli* Gene Deletion Kit
301 (Gene Bridges, Germany). Homology arms, consisting of 50 bp upstream and 50 bp
302 downstream of the target gene, were used in the deletion process. The *Km*^{r} gene was
303 amplified using PCR with primers that were fused with these homology sequences and
304 introduced into strain W3110. The *Km*^{r} gene was subsequently excised from the
305 chromosome by introducing a vector expressing the FLP recombinase, which recognizes
306 FRT sequences flanking the *Km*^{r} gene. This process was repeated for the sequential
307 deletion of all four K^+ uptake transporter genes, generating a strain deficient in these
308 transporters. All PCR primers used for gene deletion mutant construction are listed in
309 Supplementary Table 2.

310 **Plasmid construction**

311 The *sll1024* DNA fragment was synthesized by Genscript Co., Ltd. (New Jersey, USA),
312 with codon optimization for *E. coli* to improve expression efficiency (Supplementary Fig.

5). For the construction of a channel gene-expressing vector, the plasmid pSTV28Km was first created by replacing the *Cm*^{r} gene in pSTV28 (Takara, Japan) with the *Km*^{r} gene. Each channel gene was then amplified by PCR and cloned into the *Bam*HI and *Sal*I sites of the pSTV28Km vector using the SLiCE method[35]. All PCR primers used for plasmid construction are listed in Supplementary Table 2.

Growth test and measurement of K^+ uptake in *E. coli*

K^+ uptake experiments in *E. coli* were performed according to previous studies with minor modifications[36]. The K^+ uptake-deficient strains were transformed with either the pSTV28Km EV, pSTV28Km-*sll1024*, or pSTV28Km-KAT1. Growth tests were conducted as described previously with slight modifications[23,37]. *E. coli* cells were preincubated in a minimal liquid medium (46 mM Na_2HPO_4, 23 mM NaH_2PO_4, 8 mM $(NH_4)_2SO_4$, 0.4 mM $MgSO_4$, 6 mM $FeSO_4$, 10 μg/mL thiamine, and 1% glucose) supplemented with 25 μg/mL kanamycin and 30 mM KCl. Cells were harvested using centrifugation (13000 × *g*, 25 °C, and 1 min) and washed twice with a minimal medium lacking KCl. The cell suspension concentration was determined by measuring optical density at 600 nm (OD_{600}). A dilution series with OD_{600} = 1.0, 0.1, 0.01, and 0.001 was prepared and spotted onto a minimal agar medium supplemented with 25 μg/mL kanamycin and varying concentrations of KCl.

The K^+ uptake assay was conducted following previously described protocols, with some modifications to suit the experimental conditions[36–38]. *E. coli* cells were cultured in a minimal liquid medium supplemented with 25 μg/mL kanamycin and 30 mM KCl at 30 °C for 24 h. Pre-cultures were inoculated into a minimal medium supplemented with 25 μg/mL kanamycin, 30 mM KCl, and 0.5 mM isopropyl β-D-1-thiogalactopyranoside (IPTG) and incubated at 30 °C for 24 h. Cells were harvested, resuspended in 150 mM

Tris-HCl (pH 8.0) containing 1 mM EDTA, and incubated at 30 °C for 24 h. After washing three times with 150 mM Tris-HCl (pH 8.0), the cell suspension was adjusted to an OD_{600} of 3.0 in the same buffer. Glucose (10 mM) was added to the suspension, which was then shaken at 25 °C for 20 min. K^+ uptake was initiated by adding 5 mM KCl at 0 min, and 1 mL of cell suspension was collected at 0, 10, 30, and 60 min. Samples were centrifuged (13000 × *g*, 25 °C, and 1 min) through silicone oil (Sigma Aldrich). The supernatant was removed, the pellet was washed twice with water, and the silicone oil was removed. The pellet was disrupted using concentrated nitric acid, and the K content was measured using inductively coupled plasma mass spectrometry (ICP-MS; PerkinElmer).

Preparation of giant *E. coli* and patch-clamp recording

The enlargement of *E. coli* cells was performed according to a previously described method with slight modifications[21]. K^+ uptake-deficient *E. coli* strains were grown in a KLB medium (1% (w/v) tryptone, 0.5% (w/v) yeast extract, 0.5% (w/v) KCl) supplemented with 25 μg/mL kanamycin until the optical density at 600 nm (OD_{600}) reached 0.8. Cells were harvested using centrifugation at 5,000 × *g* (25 °C, 1 min) and resuspended in 1 mL of SP buffer (25 mM Tris-HCl, pH 7.4, and 400 mM sucrose) containing 200 μg/mL lysozyme. The suspension was incubated at 30 °C for 15 min. After incubation, the cells were collected using centrifugation (5,000 × *g*, 1 min), and the supernatant was removed. The cells were then grown in a GP medium (2.75% Trypticase soy broth without dextrose, 10 mM $MgSO_4$, 300 mM sucrose, 50 mM KCl) supplemented with 800 μg/mL ampicillin and 25 μg/mL kanamycin and incubated at 30 °C for 15 h. The currents were recorded using the whole-cell mode, as described previously[21–23,39].

Transmission electron microscopy

Cyanobacterial cell pellets were fixed overnight at 4 °C in 3% glutaraldehyde in 0.1 M sodium cacodylate buffer (pH 6.9). Following fixation, the samples were processed for electron microscopy. Ultrathin sections were prepared using an ultramicrotome, post-stained with lead citrate, and examined using a transmission electron microscope (TEM 300, Hitachi) operating at 75 kV. This process enabled the detailed examination of the thylakoid membrane ultrastructure in both WT and Δ*sll1024* strains of *Synechocystis* sp. PCC 6803.

Figure legends

Fig. 1 Phenotypic analysis of Sll1024 in *Synechocystis* sp. PCC 6803. a, Cultures of wild-type (WT) and Δ*sll1024* under 70 μmol photons m^{-2} s^{-1}, with photographs taken at 72 h. **b**, Localization of Sll1024 in *Synechocystis* sp. PCC 6803. Western blotting analysis of subcellular fractions from an *sll1024* expressing strain. Each lane was loaded with 50 μg of protein and probed with the antibodies indicated. Abbreviations: thylakoid membrane (Thyla), plasma membrane (Plas), soluble fraction (Sol). **c**, Photosynthetic efficiency comparison between WT and Δ*sll1024*. Measurements of total photosynthetic activity, electron transfer rate (ETR), and photosystem II activity were conducted under 1500 μmol photons m^{-2} s^{-1}. Statistic analysis was performed using a Student's *t*-test (*$p < 0.001$, **$p < 0.005$). Error bars represent mean SE (n=3).

Fig. 2 Functional analysis of Sll1024 using *E. coli* cells. a, Complementation of the K^+ uptake-deficient *E. coli* strain by Sll1024. A spot assay was performed using *E. coli* Δ4 strains harboring an empty vector (EV), Sll1024, or the *Arabidopsis* K^+ channel KAT1

on a synthetic solid medium containing 0, 15, or 30 mM KCl. Tenfold serial dilutions of cell suspensions (from 10^{-2} to 10^{-6}) were spotted and grown at 30 °C for 48 h. **b**, K^+ uptake assay: 5 mM KCl was added at t = 0 min, and K^+ content of the cells was measured over time. **c**, Patch-clamp assay: whole-cell currents elicited by voltage steps ranging from −80 to 80 mV in 10 mV increments were recorded in symmetrical 30 mM KCl, 10 mM $MgCl_2$, 10 mM Tris-MES pH 7.5, and 300 mM sorbitol. Error bars represent mean SD (n=5). **d** and **e**, Ion selectivity assay: whole-cell currents were elicited by a series of voltage steps (−80 to 80 mV) in symmetrical 100 mM KCl (○ or □), followed by replacement of extracellular KCl with 30 mM KCl (● or ■). The pipette solution contained 100 mM KCl, 10 mM $MgCl_2$, 10 mM Tris-MES pH 7.5, and 300 mM sorbitol. Error bars represent mean SE (n=3). **f** and **g**, Single channel conductance: single channel activity was recorded at membrane potentials ranging from 60 to −60 mV in 20 mV steps. **g**, Average I–V relationships of single channel currents recorded from Sll1024-expressing giant *E. coli* cells. Error bars represent mean SD (n=3).

Fig. 3 Ultrastructure of the thylakoid membrane in Δ*sll1024*. Transmission electron micrographs of *Synechocystis* sp. PCC 6803 showing representative views of the thylakoid membrane ultrastructure in wild-type (WT) (**a)** and Δ*sll1024* (**b**) cells. Enlarged views are presented below each corresponding image. **c,** Quantitative analysis of the thylakoid lumen thickness was performed using Image J software. The thickness of 39 points in the thylakoid membrane was measured in 10 wild-type cells, and the thickness at 54 points was measured in 15 Δ*sll1024* mutant cells. For the box plot, solid line indicates the median and the dotted line indicates the mean value. The top and bottom of the box indicate the 25th and 75th percentiles, respectively. Dots and whiskers represent

individual values and the spread of the data, respectively. The results depict the significant difference in lumen thickness between WT and Δ*sll1024* cells, with statistical significance indicated using Student's *t*-test (*$p < 0.001$).

Supplementary Fig. 1 Phylogenetic tree of Sll1024 homologs in cyanobacteria. The bestrophin channel Sll1024 homologs are conserved across a wide range of cyanobacterial genera and orders. A phylogenetic tree was constructed using MEGA11 software to illustrate the evolutionary relationships among Sll1024 homologs in representative cyanobacteria.

Supplementary Fig. 2 | General characteristics of Sll1024. a, Sequence alignment between Sll1024 and *Klebsiella pneumoniae* KpBest1. **b**, Hydropathy plots for Sll1024 were generated using the Kyte and Doolittle method. **c**, Ribbon diagrams of Sll1024 (left) and KpBest1 (right) depict their 3D structures, with the Sll1024 structure predicted using the AlphaFold Protein Structure Database. Key amino acid residues critical for ion selectivity in KpBest1 (I62, I66, and F70) and their corresponding residues in Sll1024 (I66, I70, and F74) are highlighted.

Supplementary Fig. 3 | Schematic representation of the *sll1024* deletion and His-tag fusion in *Synechocystis* sp. PCC 6803. a, A Cm resistance cassette was inserted into the *sll1024* gene (upper panel). Agarose gel electrophoresis of PCR products amplified from genomic DNA of WT and Δ*sll1024* strains confirmed the complete segregation of the mutant (bottom panel). **b**, A His-tag sequence and Km resistance cassette were inserted

upstream of the *sll1024* stop codon (upper panel). PCR confirmed the correct insertion, with complete segregation of the transformant (bottom panel).

Supplementary Fig. 4 | DNA sequence of *sll1024* conserved in the genomic DNA of *Synechocystis* sp. PCC 6803 and the codon-optimized DNA sequence for *E. coli*. *sll1024N*: DNA sequence of *sll1024* conserved in *Synechocystis* sp. PCC 6803. *sll1024E*: Codon-optimized DNA sequence of *sll1024* for expression in *E. coli*.

Supplementary Fig. 5 | Transmission electron micrographs of *Synechocystis* sp. PCC 6803. Transmission electron micrographs confirming the reproducibility of data shown in Fig. 3. The experimental conditions are identical to those in Fig. 3. **a**, wild-type and **b**, Δ*sll1024*.

Supplementary Fig. 6 | Possible mechanism and physiological role of Sll1024. Sll1024 enhances the efficiency of electron transfer between photosystems II and I in the electron transport system of the thylakoid membranes, contributing to the regulation of photosynthetic activity.

Data availability

The data that support the findings of this study are available from the corresponding authors on request.

References

1. Allen, J. F. Photosynthesis of ATP— Electrons, proton pumps, rotors, and poise. *Cell* **110**, 273–276 (2002).

2. Mitchell, P. Coupling of phosphorylation to electron and hydrogen transfer by a chemi-osmotic type of mechanism. *Nature* **191**, 144–148 (1961).

3. Pospíšil, P. Production of reactive oxygen species by photosystem II. *Biochim. Biophys. Acta Bioenerg.* **1787**, 1151–1160 (2009).

4. Müller, P., Li, X. P. & Niyogi, K. K. Non-photochemical quenching. A response to excess light energy. *Plant Physiol.* **125**, 1558–1566 (2001).

5. Armbruster, U. *et al.* Ion antiport accelerates photosynthetic acclimation in fluctuating light environments. *Nat. Commun.* **5**, 1–8 (2014).

6. Wang, C. *et al.* Fine-tuned regulation of the K^+/H^+ antiporter KEA3 is required to optimize photosynthesis during induction. *Plant J.* 540–553 (2017) https://doi.org/10.1111/tpj.13405.

7. Herdean, A. *et al.* A voltage-dependent chloride channel fine-tunes photosynthesis in plants. *Nat. Commun.* **7**, (2016).

8. Dukic, E. *et al.* K^+ and Cl^- channels/transporters independently fine-tune photosynthesis in plants. *Sci. Rep.* **9**, 8639 (2019).

9. Milenkovic, V. M., Langmann, T., Schreiber, R., Kunzelmann, K. & Weber, B. H. F. Molecular evolution and functional divergence of the bestrophin protein family. *BMC Evol. Biol.* **8**, 1–10 (2008).

10. Duan, Z. *et al.* A bestrophin-like protein modulates the proton motive force across the thylakoid membrane in *Arabidopsis*. *J. Integr. Plant Biol.* **58**, 848–858 (2016).

11. Yang, T. *et al.* Structure and selectivity in bestrophin ion channels. *Science* **346**, 355–359 (2014).

12. Ji, C. *et al.* Dual Ca^{2+}-dependent gates in human Bestrophin1 underlie disease-causing mechanisms of gain-of-function mutations. *Commun. Biol.* **2**, 1–13 (2019).

13. Zhang, Y. *et al.* ATP activates bestrophin ion channels through direct interaction. *Nat. Commun.* **9**, (2018).

14. Berry, S. *et al.* Potassium uptake in the unicellular cyanobacterium *Synechocystis* sp. strain PCC 6803 mainly depends on a Ktr-like system encoded by *slr1509* (*ntpJ*). *FEBS Lett.* **548**, 53–58 (2003).

15. Matsuda, N. *et al.* Na^+-dependent K^+ uptake Ktr system from the cyanobacterium *Synechocystis* sp. PCC 6803 and its role in the early phases of cell adaptation to hyperosmotic shock. *J. Biol. Chem.* **279**, 54952–54962 (2004).

16. Zanetti, M. *et al.* A novel potassium channel in photosynthetic cyanobacteria. *PLoS One* **5**, 1–10 (2010).

17. Checchetto, V. *et al.* Thylakoid potassium channel is required for efficient photosynthesis in cyanobacteria. *Proc. Natl. Acad. Sci. U. S. A.* **109**, 11043–11048 (2012).

18. Hamamoto, S. *et al.* Characterization of a tobacco TPK-type K^+ channel as a novel tonoplast K^+ channel using yeast tonoplasts. *J. Biol. Chem.* **283**, 1911–1920 (2008).

19. Bossemeyer, D., Schlosser, A. & Bakker, E. P. Specific cesium transport via the *Escherichia coli* Kup (TrkD) K^+ uptake system. *J. Bacteriol.* **171**, 2219–2221 (1989).

20. Dosch, D. C., Helmer, G. L., Sutton, S. H., Salvacion, F. F. & Epstein, W. Genetic analysis of potassium transport loci in *Escherichia coli*: Evidence for three constitutive systems mediating uptake of potassium. *J. Bacteriol.* **173**, 687–696 (1991).

21. Kuroda, T. *et al.* Patch clamp studies on ion pumps of the cytoplasmic membrane of *Escherichia coli*. *J. Biol. Chem.* **273**, 16897–16904 (1998).

22. Hamamoto, S., Mori, Y., Yabe, I. & Uozumi, N. *In vitro* and *in vivo* characterization of modulation of the vacuolar cation channel TRPY1 from *Saccharomyces cerevisiae*. *FEBS J.* 1–16 (2018) https://doi.org/10.1111/febs.14399.

23. Hamamoto, S. *et al.* Characterization of a tobacco TPK-type K^+ channel as a novel tonoplast K^+ channel using yeast tonoplasts. *J. Biol. Chem.* **283**, 1911–1920 (2008).

24. Hagino, T. *et al.* Cryo-EM structures of thylakoid-located voltage-dependent chloride channel VCCN1. *Nat. Commun.* **13**, 2505 (2022).

25. Hind, G., Nakatani, H. Y. & Izawa, S. Light-dependent redistribution of ions in suspensions of chloroplast thylakoid membranes. *Proc. Natl. Acad. Sci. U. S. A.* **71**, 1484–1488 (1974).

26. Tester, M. & Blatt, M. R. Direct measurement of K^+ channels in thylakoid membranes by incorporation of vesicles into planar lipid bilayers. *Plant Physiol.* **91**, 249–252 (1989).

27. Hinnah, S. C. & Wagner, R. Thylakoid membranes contain a high-conductance channel. *Eur. J. Biochem.* **253**, 606–613 (1998).

28. Li, M. *et al.* Impact of ion fluxes across thylakoid membranes on photosynthetic electron transport and photoprotection. *Nat. Plants* **7**, 979–988 (2021).

29. Demmig-Adams, B., Muller, O., Stewart, J. J., Cohu, C. M. & Adams, W. W. Chloroplast thylakoid structure in evergreen leaves employing strong thermal energy dissipation. *J. Photochem. Photobiol. B Biol.* **152**, 357–366 (2015).

30. Kirchhoff, H. *et al.* Dynamic control of protein diffusion within the granal thylakoid lumen. *Proc. Natl. Acad. Sci. U. S. A.* **108**, 20248–20253 (2011).

31. Tsabari, O. *et al.* Differential effects of ambient or diminished CO_2 and O_2 levels on thylakoid membrane structure in light-stressed plants. *Plant J.* **81**, 884–894 (2015).

32. Jimbo, H. *et al.* Oxidation of translation factor EF-Tu inhibits the repair of photosystem II. *Plant Physiol.* **176**, 2691–2699 (2018).

33. Jimbo, H. *et al.* Membrane lipid remodeling is required for photosystem II function under low CO_2. *Plant J.* **105**, 245–253 (2021).

34. Kusama, Y. *et al.* Zeaxanthin and echinenone protect the repair of photosystem II from inhibition by singlet oxygen in *Synechocystis* sp. PCC 6803. *Plant Cell Physiol.* **56**, 906–916 (2015).

35. Okegawa, Y. & Motohashi, K. Evaluation of seamless ligation cloning extract preparation methods from an *Escherichia coli* laboratory strain. *Anal. Biochem.* **486**, 51–53 (2015).

36. Tholema, N., Bakker, E. P., Suzuki, A. & Nakamura, T. Change to alanine of one out of four selectivity filter glycines in KtrB causes a two orders of magnitude decrease in the affinities for both K^+ and Na^+ of the Na^+-dependent K^+ uptake system KtrAB from *Vibrio alginolyticus*. *FEBS Lett.* **450**, 217–220 (1999).

37. Matsuda, N. *et al.* Na^+-dependent K^+ uptake Ktr system from the cyanobacterium *Synechocystis* sp. PCC 6803 and its role in the early phases of cell adaptation to hyperosmotic shock. *J. Biol. Chem.* **279**, 54952–54962 (2004).

38. Tanudjaja, E., Hoshi, N., Su, Y., Hamamoto, S. & Uozumi, N. Kup-mediated Cs^+ uptake and Kdp-driven K^+ uptake coordinate to promote cell growth during excess Cs^+ conditions in *Escherichia coli*. *Sci. Rep.* **7**, 2122 (2017).

39. Yabe, I. *et al.* Patch clamp studies on V-type ATPase of vacuolar membrane of haploid *Saccharomyces cerevisiae*. *J. Biol. Chem.* **274**, 34903–34910 (2002).

Acknowledgments: We thank all members of our groups and Dr. Makoto Nishiyama for the encouragement and helpful discussions. This work has been supported by grant in aid from IFO, Institute for Fermentation, Osaka to H. K. This research was also supported by Japan Society for the Promotion of Science KAKENHI grant 19K05823 and 22K05425 to S. H.

Author contributions:

S.H. and H.K. planned the project and designed the research. S.H., H.J., K.M. and K.T. performed the experiments. S.H., H.J., K.M. K.T., K.T. and H.K performed the data analysis. S.H. wrote the manuscript.

Competing interests:

The authors declare no competing financial interests.

Additional information

Extended data is available for this paper at https://doi.org/xxx.

Supplementary information The online version contains supplementary material available at https://doi.org/xxx.

Correspondence and requests for materials should be addressed to

574 Hisashi Kawasaki or Shin Hamamoto.

575 Table S1. A list of Sll1024 orthologs conserved across various cyanobacterial orders.

Order	Strain name	Accession
Acaryochloridales	*Thermosynechococcus elongatus BP-1*	WP_011058043.1
Chroococcales	*Crocosphaera subtropica ATCC 51142*	WP_009544853.1
	Crocosphaera watsonii WH 8501	WP_007305935.1
	Cyanobacterium aponinum PCC 10605	WP_015220894.1
	Xenococcus sp. PCC 7305	WP_006510562.1
Chroococcidiopsidales	*Gloeocapsa sp. PCC 7428*	WP_015190873.1
Gloeomargarita	*Gloeomargarita lithophora D10*	WP_071454716.1
Nostocales	*Anabaena cylindrica PCC 7122*	WP_015216280.1
	Calothrix sp. PCC 7103	WP_026093107.1
	Chlorogloeopsis fritschii PCC 6912	WP_016875612.1
	Cylindrospermum stagnale PCC 7417	WP_015206675.1
	Fischerella sp. PCC 9605	WP_026734180.1
	Fortiea contorta PCC 7126	WP_017651421.1
	Mastigocladopsis repens PCC 10914	WP_017318703.1
	Mastigocoleus testarum BC008	WP_027837716.1
	Nostoc punctiforme ATCC 29133; PCC 73	WP_012411391.1
	Nostoc sp. PCC 7120	WP_010997138.1
	Scytonema hoffmannii PCC 7110	WP_033334745.1
	Tolypothrix sp. PCC 7601 = UTEX B 481	WP_045872692.1
	Trichormus variabilis ATCC 29413	WP_011317776.1
Oscillatoriales	*Crinalium epipsammum PCC 9333*	WP_015202361.1
	Lyngbya sp. PCC 8106	WP_009786460.1
	Microcoleus sp. PCC 7113	WP_015184108.1
	Microcoleus vaginatus FGP-2	WP_006631076.1
	Oscillatoria sp. PCC 10802	WP_017719381.1
	Phormidium tenue NIES-30	WP_084173102.1
	Planktothrix rubescens NIVA-CYA 407	WP_043937957.1
	Trichodesmium erythraeum IMS101	WP_011612764.1
Pleurocapsales	*Pleurocapsa sp. PCC 7319*	WP_019506635.1
Prochlorotrichales	*Prochlorothrix hollandica PCC 9006*	WP_046492898.1
Spirulinales	*Spirulina major PCC 6313*	WP_217650504.1
Synechococcales	*Acaryochloris marina MBIC11017*	WP_012165290.1
	Chamaesiphon minutus PCC 6605	WP_232432130.1
	Leptolyngbya boryana PCC 6306	WP_017286932.1

	Leptolyngbya sp. PCC 6406	WP_008314573.1
	Pseudanabaena sp. PCC 6802	WP_019498265.1
	Synechococcus elongatus PCC 7942	WP_011377641.1
	Synechococcus sp. JA-3-3Ab	WP_041439137.1
	Synechococcus sp. PCC 7002	WP_012306097.1
	Synechococcus sp. PCC 7336	WP_071590851.1
	Synechococcus sp. RS9916	WP_156777453.1
	Synechococcus sp. WH 8016	WP_038013999.1
	Synechocystis sp. PCC 6803	WP_228670066.1

576

577

578 Table S2. List of primers used in this study (5’ – 3’).

Primer name	Sequence
F1	TTGAGCAAATTCTTGAGCTTTTTCA
R1	TCCGGCAACAGAGCCCAAAT
F2	ATCCGGTTACCGGAAGCTT
R2	TCAGGGCAACGGTTTAGCC
F3	CCGAGTTGTAGTCGGCAGTC
R3	GACGTCTGTATTAACGAAGC
R4	GGCATGGAGGACATACTAGTGGTGGTGGTGGTGGTGGTC CCCATGGGAGATCT
F5	GATTACGAATTCCCCTGTTTATTCATTTATCCATGTAGAAC
R5	TGCGCTGAGGCGGCACCATCTTTCT
F6	TATGTCCTCCATGCCGATTACGAATTCCCCGGATC
R6	GATTACGAATTCCCCGGATC
kdpA_ko-F	TTATTACTGGGTTATCTGGTTTATGCCCTGATCAATGCGG AGGCGTTCTGAATTAACCCTCACTAAAGGGCGG
kdpA_ko-R	CGAATAGCGCCAGTTGTTTACGACTCATATTCAGTGCTCA CTCAATATCATAATACGACTCACTATAGGGCTC
trkG_ko-F	ATAATCATAATATTGCAGCAAGGTGGTTATAATTGAAAGA ATATTTAGATAATTAACCCTCACTAAAGGGCGG
trkG_ko-R	ATGAGTGAGTCAACATAATATTAAACTCACAATTATAAAT CAGCCATATATAATACGACTCACTATAGGGCTC
trkH_ko-F	ATTGAAGAATAATCCCCACTTCGTTTTGCAGAACTAAGG AAGCGGCAGAGAATTAACCCTCACTAAAGGGCGG
trkH_ko-R	TTGTCCGTCCCTTGTTGAGAAAAGAATTAATGTTTTCAC GTATTACTCCATAATACGACTCACTATAGGGCTC
kup_ko-F	TGGGCCAAGGGACTAAGCACACATTTCATATTTCAACGA AAGACTAGTCTAATTAACCCTCACTAAAGGGCGG
kup_ko-R	TAACCATGAAAACAAAAACGCCCCCTTATGAAGAAAGG AGGCGTCTGGCGTAATACGACTCACTATAGGGCTC
Sll1024pSTV28Km-F	TCGAGCTCGGTACCCGGGTGAGGATCCATGAGCTTCTTT AGCCAC

Sll1024pSTV28Km-R	AGATTTTGAGACACAACGTCGACTTAGTCGCCGTGGCTAATCTG
KAT1pSTV28Km-F	TCGAGCTCGGTACCCGGGTGAGGATCCATGTCGATCTCTTGGACTCG
KAT1pSTV28Km-R	AGATTTTGAGACACAACGTCGACTCAATTTGATGAAAAATAC

579

Figure 1

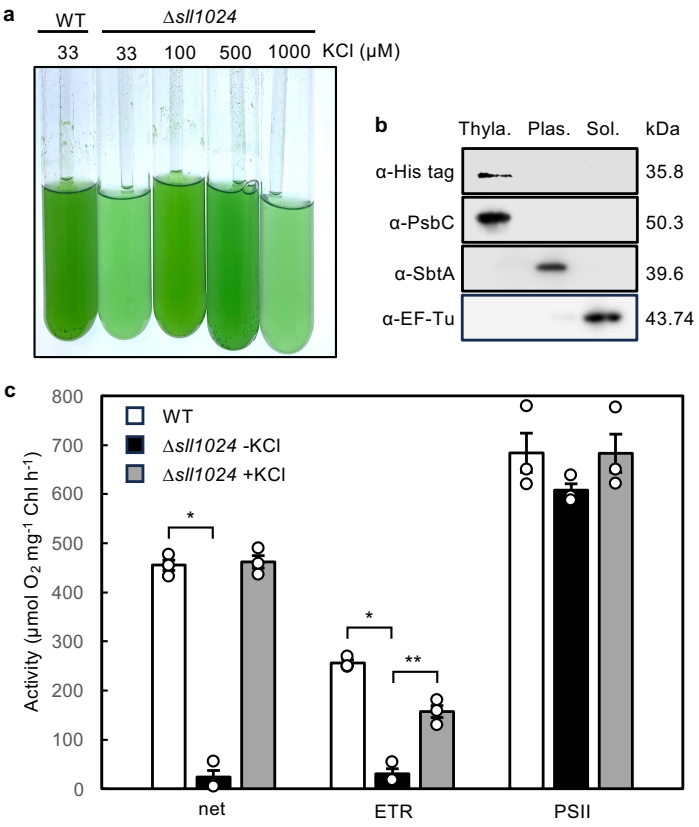

a
WT
Δsll1024
33
33
100
500
1000
KCl (μM)
b
Thyla.
Plas.
Sol.
kDa
α-His tag
35.8
α-PsbC
50.3
α-SbtA
39.6
α-EF-Tu
43.74
c
WT
Δsll1024 -KCl
Δsll1024 +KCl
Activity (μmol O2 mg-1 Chl h-1)
800
700
600
500
400
300
200
100
0
*
*
**
net
ETR
PSII

Figure 2

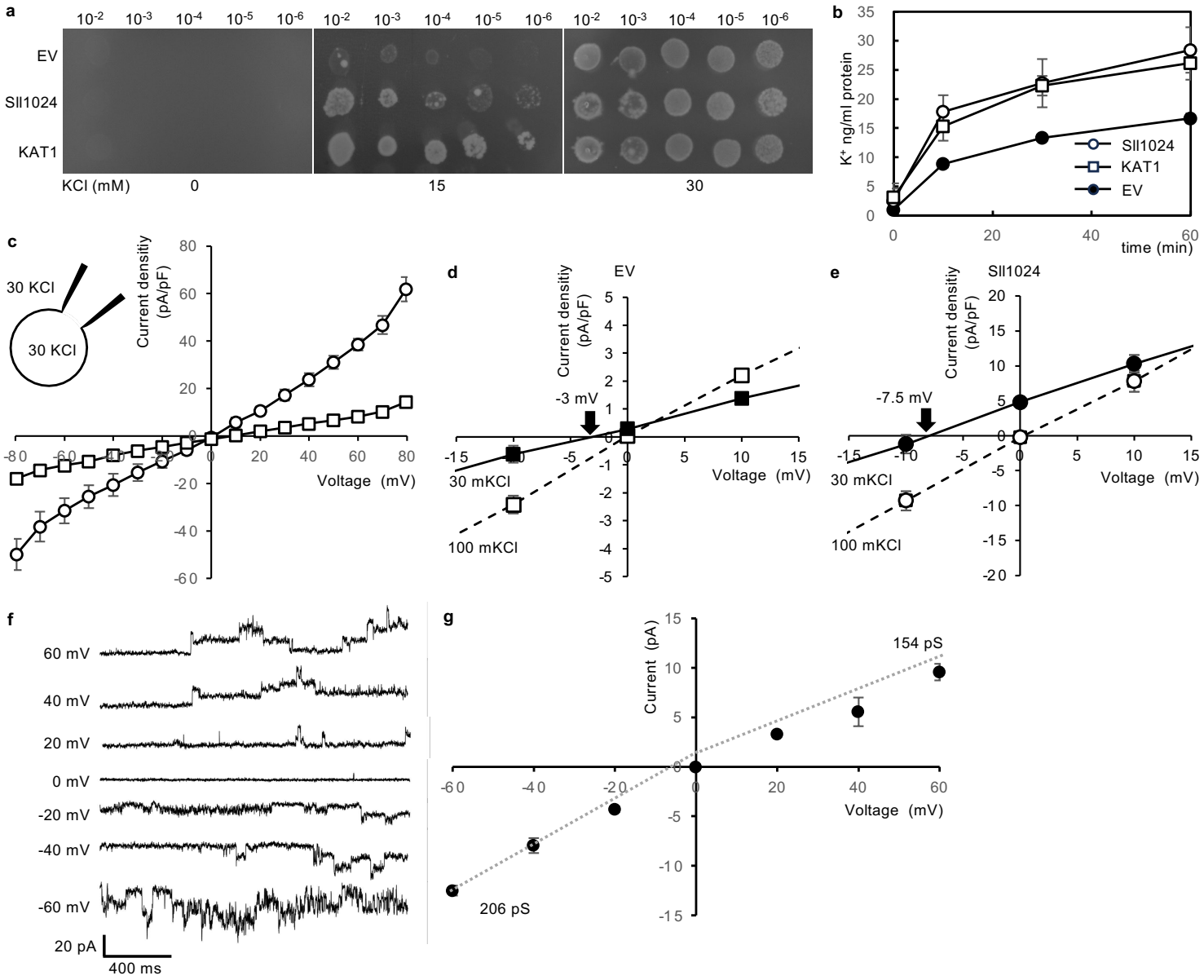
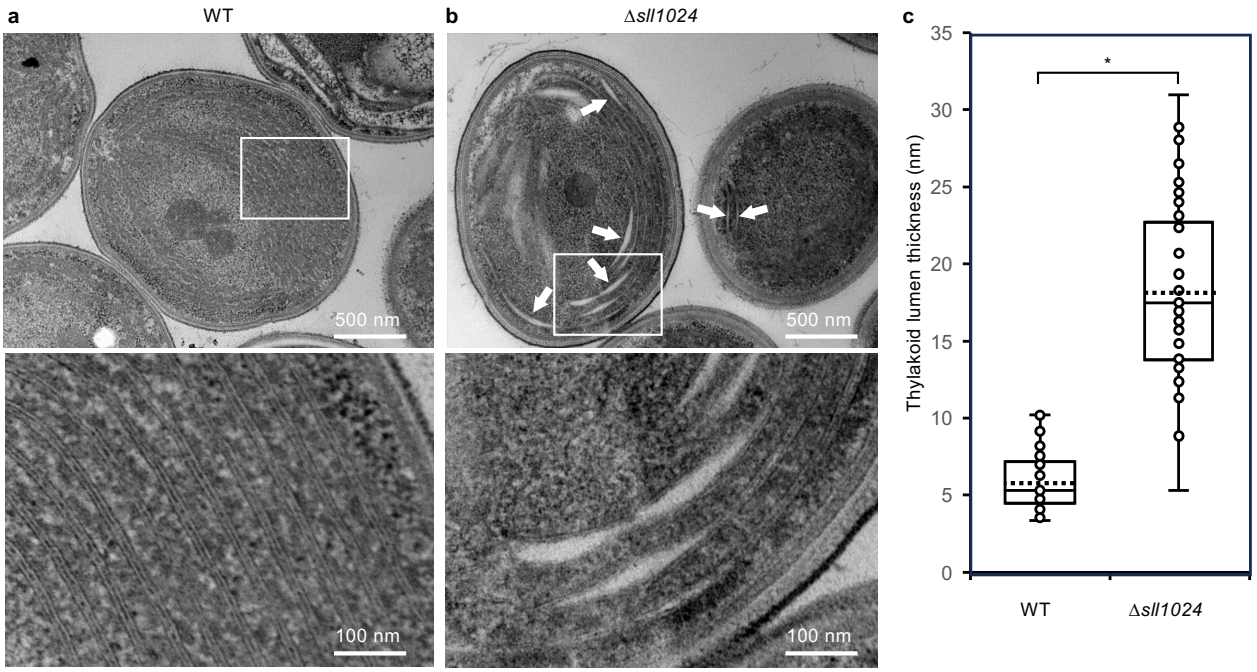
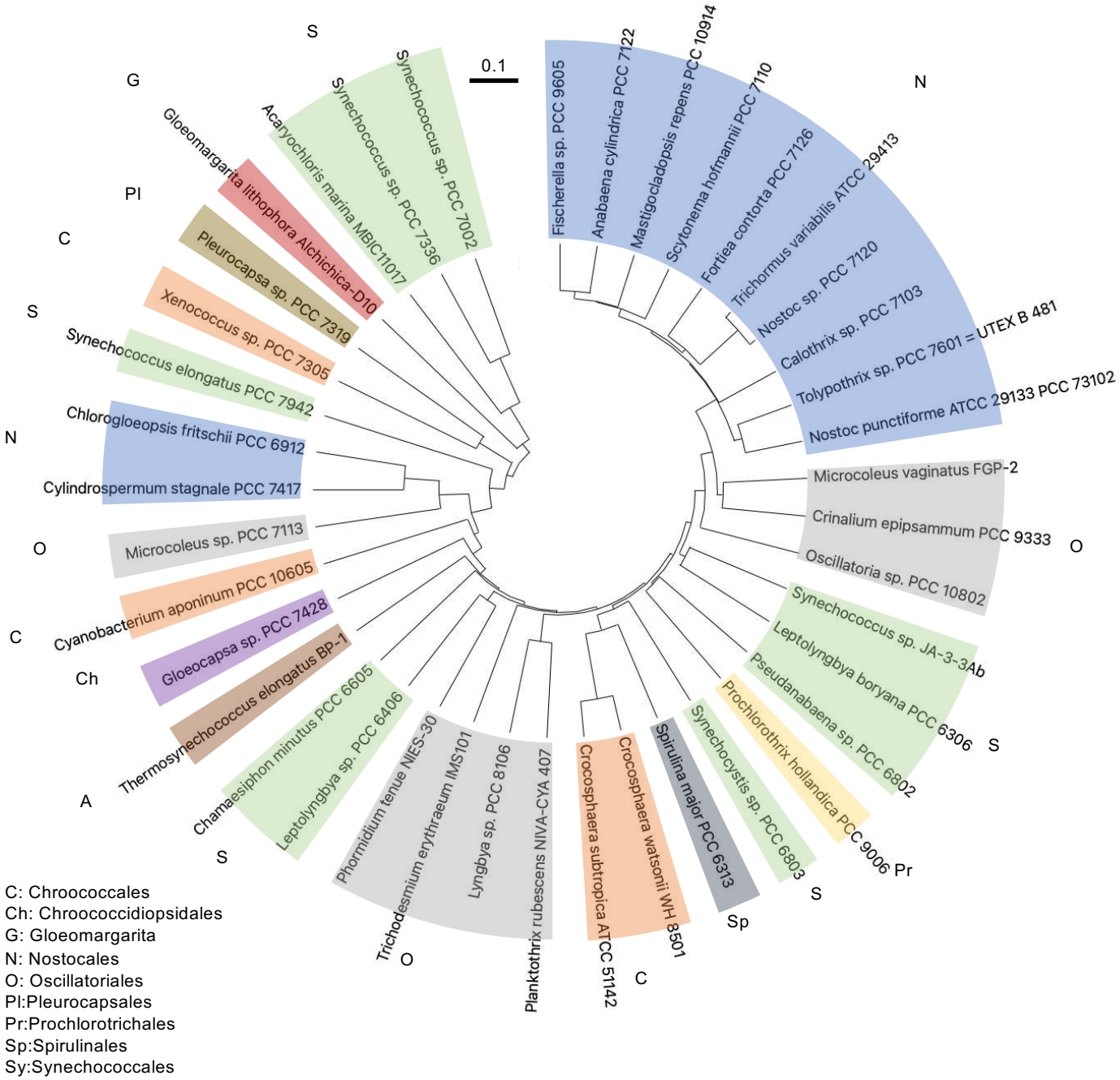

a
10-2 10-3 10-4 10-5 10-6 10-2 10-3 10-4 10-5 10-6 10-2 10-3 10-4 10-5 10-6
EV
SII1024
KAT1
KCl (mM) 0 15 30
b
K+ ng/ml protein
time (min)
SII1024
KAT1
EV
c
30 KCl
30 KCl
Current density (pA/pF)
Voltage (mV)
d
EV
Current density (pA/pF)
-3 mV
30 mKCl
100 mKCl
Voltage (mV)
e
SII1024
Current density (pA/pF)
-7.5 mV
30 mKCl
100 mKCl
Voltage (mV)
f
60 mV
40 mV
20 mV
0 mV
-20 mV
-40 mV
-60 mV
20 pA
400 ms
g
Current (pA)
154 pS
206 pS
Voltage (mV)

Figure 3

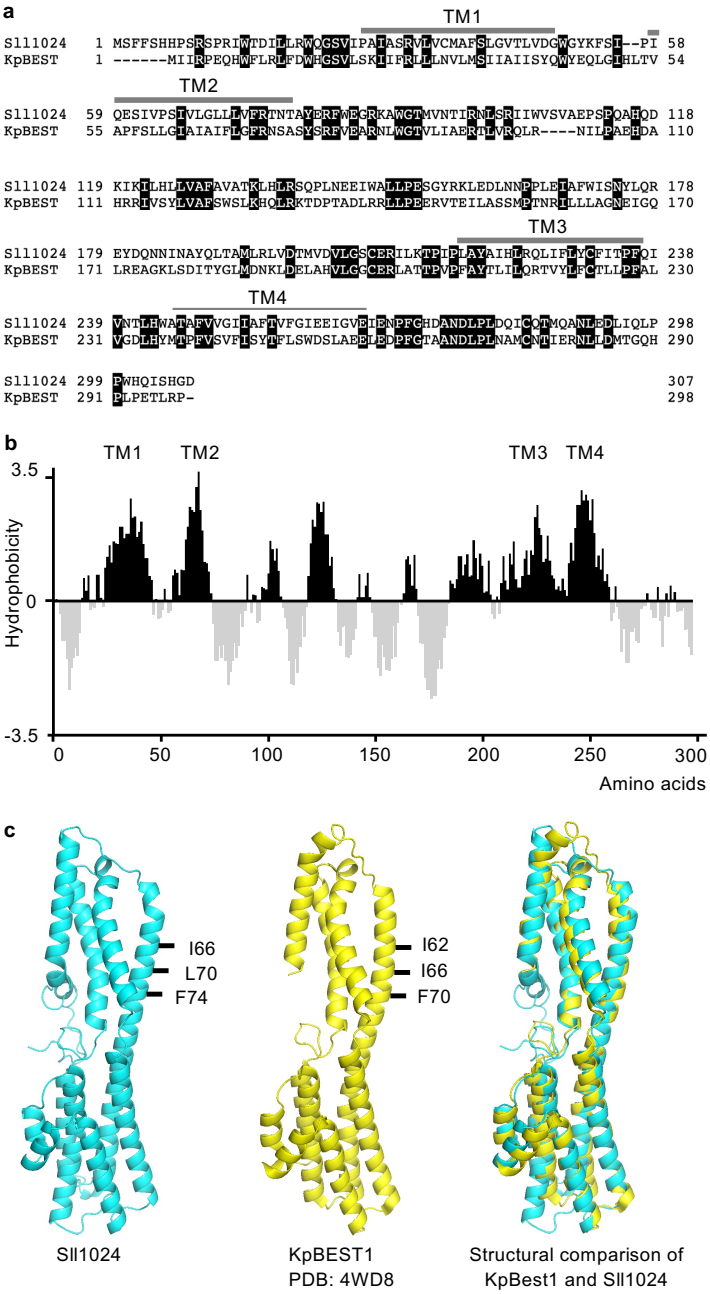

a
WT
b
Δsll1024
500 nm
500 nm
100 nm
100 nm
c
Thylakoid lumen thickness (nm)
35
30
25
20
15
10
5
0
*
WT
Δsll1024

Supplemental Figure 1

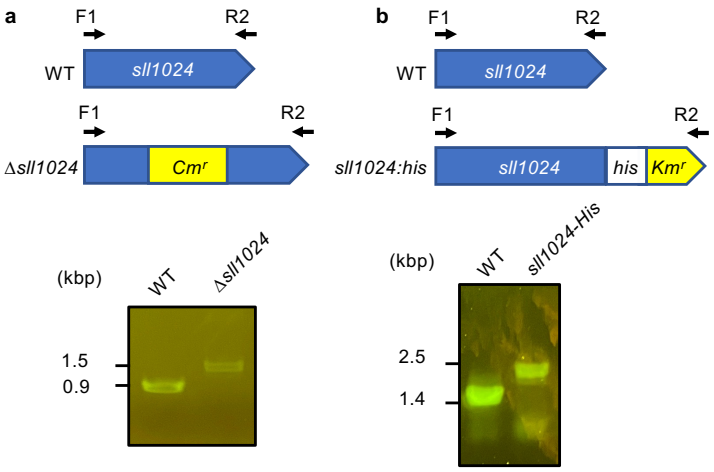


C: Chroococcales
Ch: Chroococcidiopsidales
G: Gloeomargarita
N: Nostocales
O: Oscillatoriales
Pl:Pleurocapsales
Pr:Prochlorotrichales
Sp:Spirulinales
Sy:Synechococcales

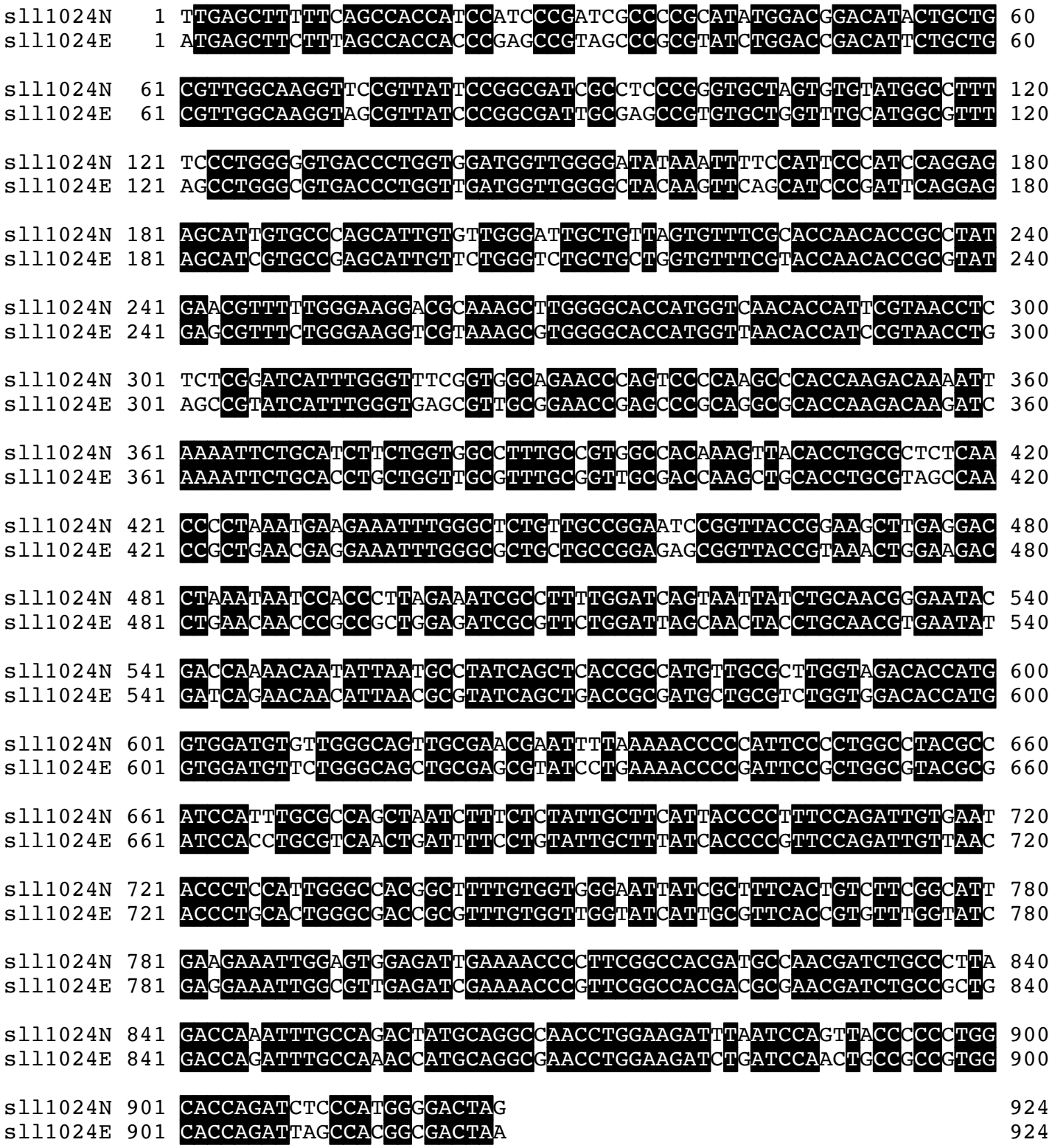
Supplemental Figure 2



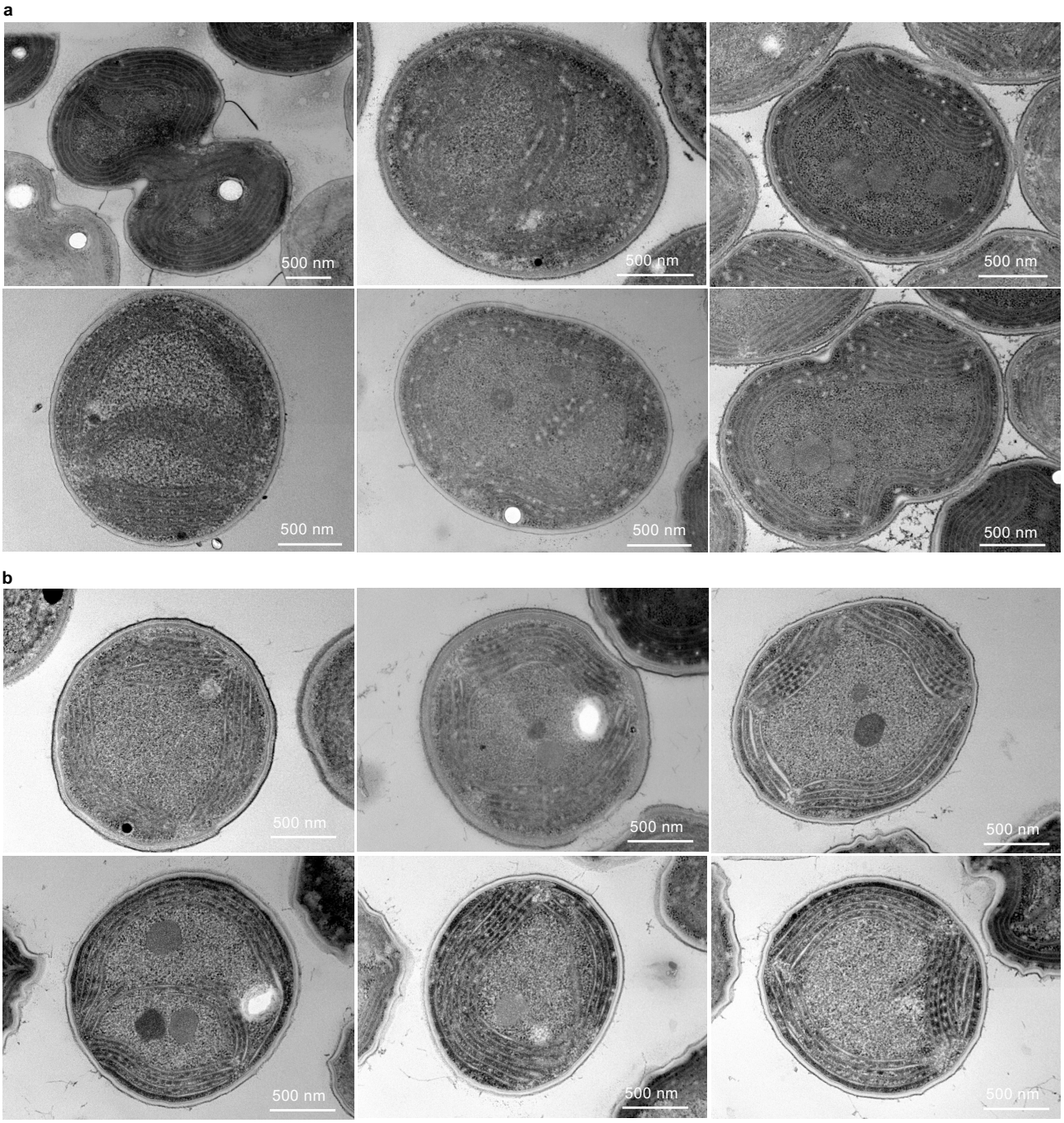
Supplemental Figure 3



Supplemental Figure 4



Supplemental Figure 5



Supplemental Figure 6

